A COMPUTATIONALLY EFFICIENT MODELLING OF LAMINAR SEPARATION BUBBLES

Paolo Dini and Mark D. Maughmer
Department of Aerospace Engineering
The Pennsylvania State University, University Park, Pennsylvania

Introduction

In order to predict the aerodynamic characteristics of airfoils operating at low Reynolds numbers ($R < 5.0 \times 10^5$), it is necessary to accurately account for the effects of laminar (transitional) separation bubbles.[1] In general, the greatest difficulty comes about when attempting to determine the increase in profile drag that results from the presence of separation bubbles. Because the drag on an airfoil depends on the trailing-edge value of the momentum thickness,[2] the increase in drag that accompanies separation bubbles is primarily due to the rapid increase in momentum thickness that occurs in a bubble compared to the much smaller growth that occurs with a natural transition from a laminar to a turbulent boundary layer. As a consequence, when a separation bubble is the actual mechanism of transition, methods that assume transition occurs at the laminar separation point and use the boundary-layer properties at that point as the initial conditions for the turbulent boundary-layer calculations usually underpredict the drag. Thus, to successfully determine the increase in drag on an airfoil due to separation bubbles, it is necessary to accurately model the development of the boundary layer through the bubble.

While a number of empirically based separation bubble models have been introduced in the past, some of which are detailed in Ref. 3, the majority of these assume that the bubble development is fully predictable from upstream conditions. More recently, much more accurate predictions have been made possible using viscous/inviscid interaction approaches such as those described in Refs. 4-6. By such means, the influence of the bubble on the entire velocity distribution over the airfoil is accounted for globally by iterating between the inviscid flow and boundary-layer solutions. While not of much concern in predicting the aerodynamic characteristics of a single airfoil, the amount of computational time required for such boundary-layer iteration methods becomes consequential in the case of airfoil design for which the number of analysis cases required can become very large.

One way of accounting for laminar separation bubbles in airfoil design is the bubble analog used in the design and analysis program of Eppler and Somers.[7,8] In this method, the designer is warned about the presence of separation bubbles which might unacceptably increase the drag over that which is predicted assuming that transition occurs at laminar separation. Although this approach has proven very useful in designing airfoils for low Reynolds number applications, it would be advantageous to have predictions of section properties which more fully account for the presence of laminar separation bubbles provided this can be done without significantly increasing the computational time. Toward this end, a locally interactive separation bubble model has been developed and incorporated into the Eppler and Somers program. Although unable to account for strong interactions such as the large reduction in suction peak sometimes caused by leading-edge bubbles, it is able to predict the increase in drag and the local alteration

of the airfoil pressure distribution that is caused by bubbles occurring in the operational range which is of most interest.

To fully determine the behavior and influence of a laminar separation bubble, it is necessary to accurately predict the shear-layer development in the regions of the laminar separation bubble indicated in Fig. 1. The formation of a bubble is initiatated at point S, shown in the figure, by the laminar boundary layer separating from the airfoil surface. Using integral boundary-layer methods, this point can be determined with the accuracy needed for airfoil design work. Once separated, the free shear layer development must be tracked and the transition from laminar to turbulent flow, which occurs near the point T, predicted. As shown in Fig. 2, the separation bubble causes a plateau to form in the velocity distribution between the points corresponding to laminar separation and the end of the transition region. From this point, the turbulent part of the bubble encompasses a pressure recovery region which leads to the reattachment of the turbulent shear layer at point R. As an additional pressure recovery always occurs downstream of a reattachment point, the velocity distribution corresponding to the highly non-equilibrium, relaxing boundary layer downstream of reattachment "undershoots" the inviscid distribution. Eventually, the turbulent boundary layer reaches its fully-developed state and the undershoot region merges smoothly from below with the inviscid velocity distribution. Clearly it is possible, especially at low Reynolds numbers, that the turbulent boundary layer never reaches equilibrium before the trailing edge of the airfoil.

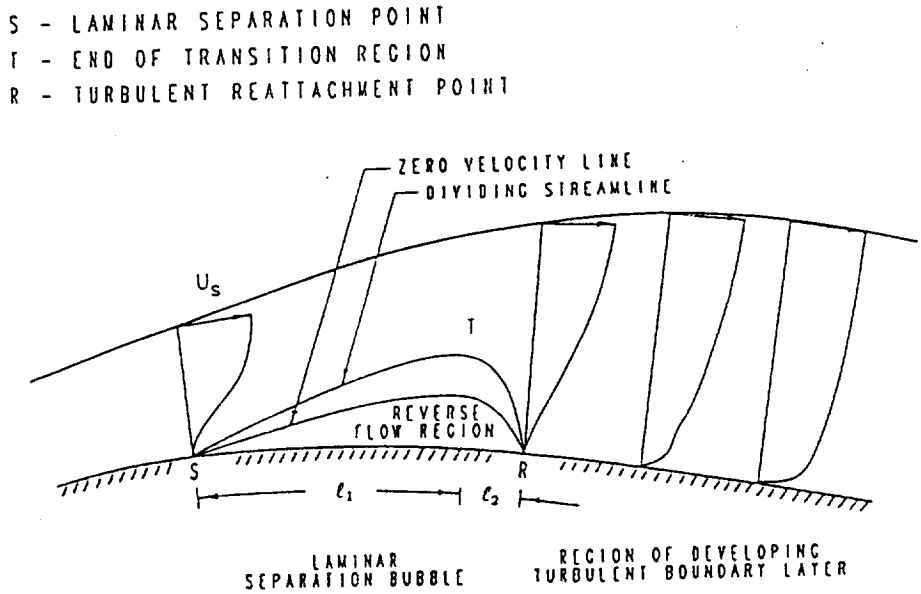

Fig. 1: Sectional view of a two-dimensional short laminar separation bubble.

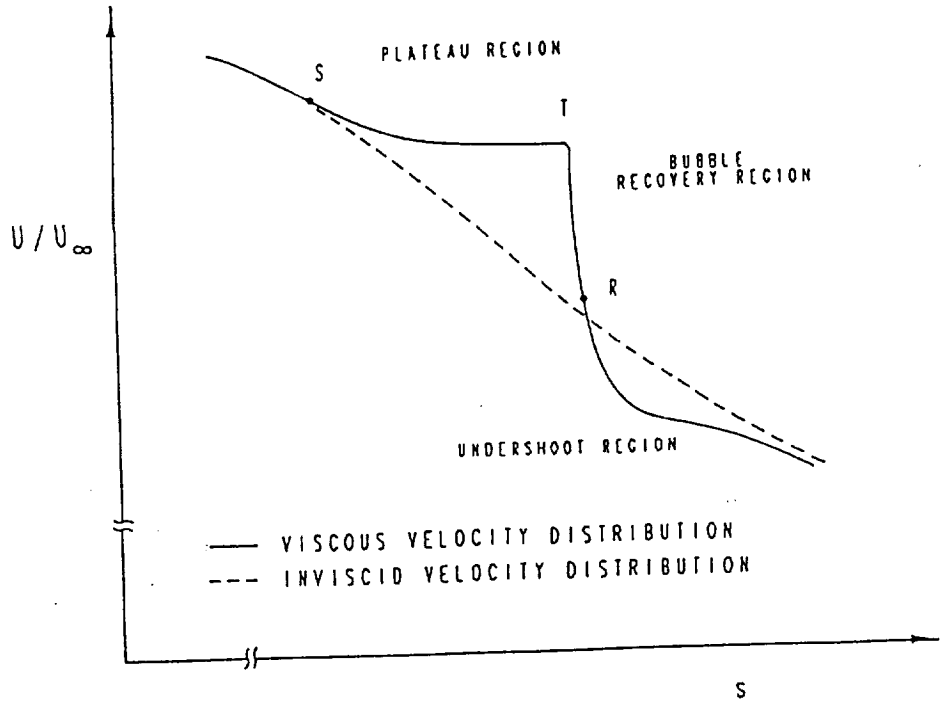

Fig. 2: Influence of a short laminar separation bubble on the velocity distribution over an airfoil.

Overview of Procedure for Modelling Laminar Separation Bubbles

Efforts to develop a method able to predict the effects of a laminar separation bubble which interacts weakly with the inviscid flow, the so-called short bubble, began with the incorporation of the classical empirical model of Horton,[9] modified according to the suggestions of Roberts[10] and Schmidt,[3] into the Eppler and Somers program. Because they are formulated in terms of integral boundary-layer properties, bubble models such as these are well suited to the integral boundary-layer analysis employed by Eppler. Specifically, this method makes use of the momentum and energy integral equations,

$$\frac{d\delta_2}{ds} = \frac{c_f}{2} - (H_{12} + 2)\frac{\delta_2}{U}\frac{dU}{ds} \tag{1}$$

$$\frac{d\delta_3}{ds} = C_D - 3\frac{\delta_3}{U}\frac{dU}{ds} \tag{2}$$

along with the appropriate closure relations.[11]

Using the empirical separation bubble model noted, the sensitivity of the boundary-layer development and drag prediction to various parts of the bubble was explored. As detailed in Refs. 12 and 13, and reported by other researchers as well,[14] it is found that the bubble development for such models is very sensitive to small variations in the governing parameters. Thus, although generally accurate for predicting features of the bubble to within twenty percent, empirical bubble models based only on upstream conditions are not able of providing acceptable drag predictions. Consequently, it was concluded that the accuracy desired could be achieved only by a model which accounts for the effects of the downstream portions of the bubble on those upstream. In particular, along with the chord Reynolds number and the upstream development

of the laminar boundary layer, the development of the bubble is found to depend strongly on the total amount of pressure which is to be recovered along the bubble. These variable flow characteristics scale well with two dimensionless quantities, the Reynolds number based on momentum thickness at the laminar separation point, $(R_{\delta_2})_S$, and Gaster's pressure gradient parameter,[15]

$$P = \frac{[(\delta_2)_S]^2}{\nu}\frac{\Delta U}{\Delta s} = R\left[\frac{(\delta_2)_S}{c}\right]^2 \frac{\Delta(U/U_\infty)}{\Delta(s/c)} \tag{3}$$

It should be noted that, while $(R_{\delta_2})_S$ has been used in other models to account for decreasing transition length with increasing Reynolds number, Gaster's parameter has been used in the past only as a criterion of when reattachment of the short bubble is not possible and a long bubble forms. Justification that the value of P has a strong influence on the transition process and other aspects of the bubble development, such as the velocity plateau region of the bubble, is motivated by the unsteady laminar simulation presented in Ref. 16. In this research, the criterion for the "bursting" of short bubbles is found to correlate well with the boundary between steady and unsteady reattachment of a laminar boundary layer subjected to an imposed pressure gradient. The unsteadiness is due to a periodic vortex-shedding which increases in frequency and intensity as the value of Gaster's parameter increases. In view of the ellipticity of this recirculating flow field, it is not too surprising that this frequency is found to correspond to the most unstable frequency from a linear stability analysis of the laminar free shear layer. Thus, it is expected that transition in such a flow field would be strongly dependent on the shedding frequency as is characterized by the value of Gaster's parameter. Because the short separation bubble is analogous to this unsteady reattachment process, it is reasonable that, in addition to $(R_{\delta_2})_S$, the transition process should depend on the downstream reattachment of the turbulent shear layer and the value of Gaster's pressure gradient parameter.

Starting with the inviscid velocity distribution over an airfoil, the scheme used by the present method of predicting the development of laminar separation bubbles is summarized by the flow diagram shown in Fig. 3. As indicated, the bubble model is evoked when laminar separation is predicted. At that point $(R_{\delta_2})_S$ is determined and, based on the inviscid velocity gradient at the laminar separation point, an initial estimate of Gaster's parameter, P, is made. From the separation point, the velocity distribution in the plateau region is prescribed. The function which defines this distribution depends both on P and the matching of its slope to that of the inviscid velocity distribution at the laminar separation point. Using the prescribed velocity distribution over the laminar part of the bubble, the boundary-layer development is accomplished using the momentum and energy integral equations, Eqs. (1) and (2), along with appropriate closure relationships which, as will be described, were derived using the reverse-flow velocity profiles developed by Green.[17] Likewise, these profiles were used to develop the criterion used to predict transition in the free shear layer. This criterion is also a function of $(R_{\delta_2})_S$ and P. The turbulent part of the bubble and the undershoot region are determined by prescribing the distribution of H_{32} and solving the integral boundary-layer equations in the inverse mode. At this point, a local iteration is carried out to ensure that Horton's reattachment condition[9] is satisfied for a velocity distribution in the non-equilibrium region of the bubble that merges smoothly downstream with the inviscid velocity distribution. Once this iteration has converged, a new value of P is calculated from the velocity gradient along the bubble as determined using the points of laminar separation and the point where the bubble recovery first crosses the inviscid distribution. With this new value of P, an outer iteration repeats the calculations indicated until the overall length of the bubble no longer changes. It is through the two iteration schemes that the influence of the downstream conditions in the bubble are communicated upstream.

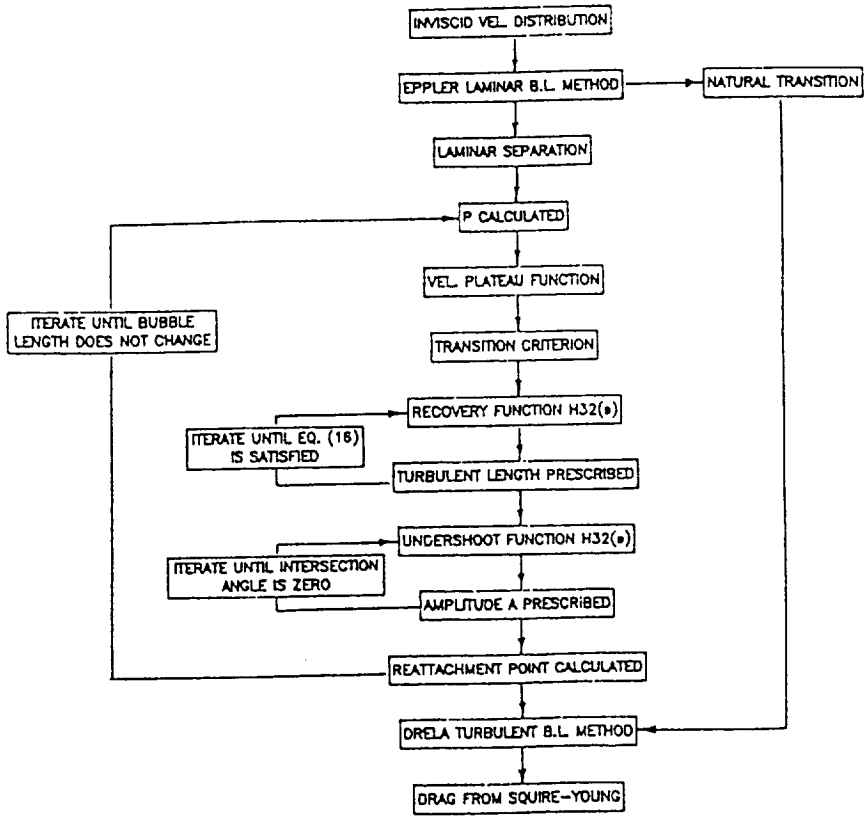

Fig. 3: Flow chart of computational scheme used to model laminar separation bubbles in the flow over airfoils.

Details of the Laminar Separation Bubble Model

In the present procedure for modelling laminar separation bubbles, the laminar closure correlations, the velocity distribution in the plateau region, transition, and the function describing the undershoot region depend only on $(R_{\delta_2})_S$ and P. All other features of the bubble are determined from the governing equations. The specific regions of the bubble model will now be described.

Laminar Part of the Bubble

The Eppler and Somers program uses a very reliable criterion to detect laminar separation, based on the value of the energy to momentum thickness shape factor,

$$(H_{32})_S = 1.515095 \tag{4}$$

This value is approached from above. Since the analysis method is formulated in the direct mode, a small error is introduced in the prediction of the laminar separation point by the presence of the Goldstein singularity. This causes the distribution of H_{32} to exhibit a very steep slope immediately upstream of separation, which is a similar behavior to that of the skin-friction coefficient. Furthermore, the direct formulation precludes any upstream influence of the bubble on the pressure distribution. In the present version of the bubble model this local interaction is neglected. Although possibly important for leading-edge bubbles, it should not have a major impact on the development of mid-chord bubbles.

Upon detection of laminar separation, the development of the separated laminar shear layer is calculated using the same governing equations, the momentum and energy integral equations, together with closure relations obtained from a family of reversed laminar velocity profiles. Instead of implementing this boundary-layer method in the inverse mode as it is usually done, the development of a family of pressure distributions in the laminar part of the bubble allows its calculation in the direct mode.

The function used to approximate the pressure distribution in the laminar part of the bubble is a generalization of that developed by van Ingen and Boermans and presented in Refs. 18 and 19,

$$\frac{U}{U_S} = .978 + .022\exp(-4.454\xi - 2.5\xi^2) \tag{5}$$

where

$$\xi = \frac{s - s_S}{(R_{\delta_2})_S(\delta_2)_S} \tag{6}$$

This distribution, unlike the constant-pressure plateau used by Horton, allows a slight pressure rise after laminar separation. Using detailed pressure distributions obtained from recent wind-tunnel tests of the NASA NLF(1)-1015 airfoil[20] in the Low-Turbulence Pressure Tunnel at the NASA Langley Research Center, the accuracy of Eq. (5) has been checked for several different conditions. It is found that, when the overall pressure gradient along the bubble decreases, the velocity distribution over the plateau region falls below that given by Eq. (5) while, when the pressure gradient steepens, it rises above. To account for this effect, Eq. (5) is rewritten as

$$\frac{U}{U_S} = (1 - DU) + DU\exp(-4.454\xi - 2.5\xi^2) \tag{7}$$

where DU is indicative of the amount of the pressure rise accomplished by the plateau velocity distribution over the laminar part of the bubble. It is found to be well represented as a function of the Gaster pressure gradient parameter, P. This functional relationship, shown in Fig. 4, was developed by extracting corresponding values of DU and P directly from the experimental pressure distributions of the NLF(1)-1015 and the Eppler E387 airfoils.[20,21] The solid line is a quadratic least-squares fit that has been included in the model,

$$DU = 0.0609691 + 0.304819P + 0.507176P^2 \tag{8}$$

It should be noted that the value of $DU = 0.022$ used by van Ingen and Boermans falls in the middle of the variation in DU shown in Fig. 4.

Upon examination of the velocity distributions obtained using Eqs. (6)-(8), it was noticed that unlike in the experimental distributions, a discontinuity in the velocity gradient at the point of laminar separation was present. Therefore, to match the gradients at laminar separation, an additional variable is introduced into the velocity distribution given by Eq. (7). Specifically, the product $[(R_{\delta_2})_S(\delta_2)_S]$ in Eq. (6) can be treated simply as a scaling factor between the physical variable, s, and the universal dimensionless variable, ξ. Consequently, the value of this scaling factor is determined as that which yields a velocity distribution in the laminar part of the bubble whose gradient is continuous with the gradient of the inviscid velocity distribution at separation.

Using the prescribed velocity distribution over the laminar part of the bubble, the development of the separated laminar shear layer is calculated by means of the same governing equations used for the rest of the boundary layer, the momentum and energy integral equations. Since δ_2 and δ_3 are obtained directly from the governing equations, the transition criterion is expressed

in terms of $(H_{32})_T$ as a function of $(R_{\delta_2})_S$ and P. A family of velocity profiles must likewise be chosen to develop the closure correlations for $H_{12}(H_{32})$, $c_f(H_{32}, R_{\delta_2})$, and $C_D(H_{32}, R_{\delta_2})$. The correlations based on the reversed Falkner-Skan, or Stewartson,[22] profiles developed by Drela[5] were originally included in the model. As discussed by Fitzgerald and Mueller,[23] however, recent measurements inside the bubble show velocity profiles that are quite different from the Stewartson profiles and closer to the two-parameter profile family originally developed by Green.[17] As shown in Fig. 5, the two parameters, h/b and G, are linked to the geometrical characteristics of the profiles. (h/b) is the ratio of the distance of the shear layer from the centerline of the wake to the width of the shear layer and G is the amplitude of the Coles wake function. Since there is slip along the centerline of such a recirculating base flow, these profiles cannot be used to develop a correlation for c_f. In view of the characteristically small values of c_f in the laminar part of the bubble, however, this should not be a problem.

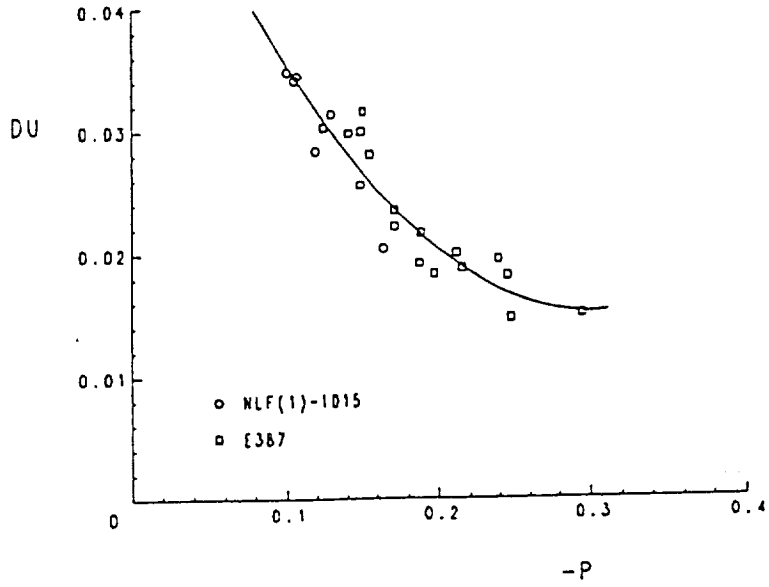

Fig. 4: Pressure recovery in the laminar part of the bubble as a function of Gaster's pressure gradient parameter. o : NLF(1)-1015 airfoil, NASA LaRC, June 1987; □ : E387 airfoil.[21]

By applying the definitions for the integral thicknesses of the boundary layer and the dissipation coefficient, relationships for H_{12}, H_{32}, and $R_{\delta_2} C_D$ as functions of h/b and G are obtained for the Green profiles. The results are shown in Figs. 6 and 7 where these new two-parameter correlations are compared to those developed by Drela from the Stewartson profiles. The solid lines utilize the fitted variations of G and (h/b). As both H_{12} and H_{32} increase monotonically between separation and transition, moving to greater values of the abscissa on these plots corresponds to moving downstream inside the bubble. Thus, both are similar to the Stewartson correlations near separation but can be quite different further downstream. It appears from the measurements that the back-flow, which is proportional to G, may be constant within each bubble although different for different bubbles. From Fig. 6, the values of shape factors actually measured, although different in absolute value, follow the same slope thus confirming a constant value of back-flow velocity. These considerations justify eliminating (h/b) between the expressions for the shape factors and expressing the closure relationships in terms of H_{32}, calculated

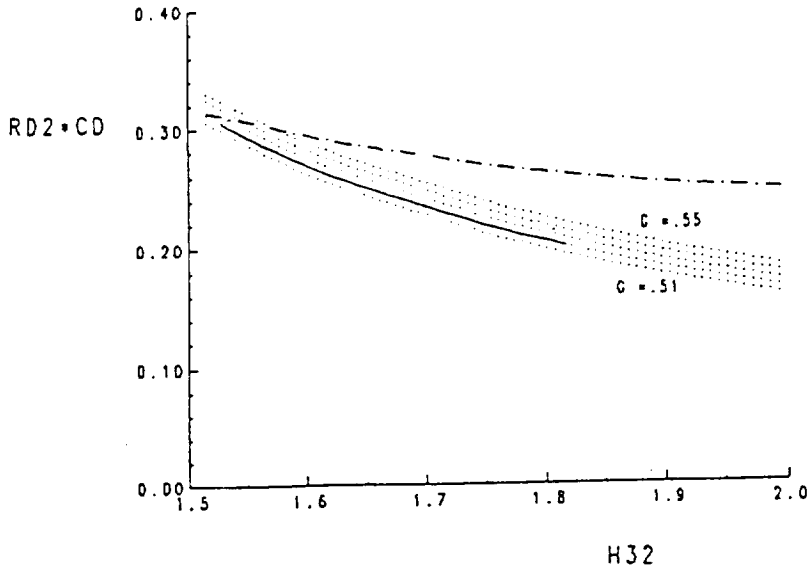

Fig. 7: Comparison of dissipation coefficient correlations. —·— : Ref. 5, from Stewartson profiles; ——— : Ref. 23, from fitted Green profiles; · · · : Eq. (10).

from the governing equations, and G, whose behavior within each bubble can be correlated to local flow conditions. Thus, the closure correlations are

$$H_{12} = \frac{3(1-G) - H_{32}}{(1-G)(1-2G)} \tag{9}$$

$$R_{\delta_2} C_D = \frac{\pi^2 G^3}{2} \left[1 - \frac{3}{2} G - \frac{(4-5G)(1-G) - (2-3G)H_{32}}{4(1-G) - 2H_{32}} \right] \tag{10}$$

The unknown quantities in the boundary-layer method for the laminar part of the bubble have been reduced to G and c_f. Physically grounded assumptions can be made about the dependence of these variables on local flow conditions. For instance, it seems reasonable to expect that, as the pressure gradient along the bubble increases, so does the strength of the recirculation and, therefore, $-c_f$. In the present version of the model, however, G is related to P such that $(\delta_2)_S$ plays an important part in determining the ratio of reverse velocity to forward boundary-layer edge velocity. The value of c_f is held constant between separation and transition.

Transition

The criterion for predicting transition in the free shear layer presently used was arrived at only after establishing that the addition of a second parameter in the laminar reversed velocity profiles still did not provide the bubble model with enough generality. The Green profiles correlations have been retained, however, as the present form of the transition criterion is believed to embody both the stability characteristics of free shear layers of varying velocity ratios (varying amounts of back-flow) as well as the perhaps more important input from the unsteady reattaching turbulent shear layer.

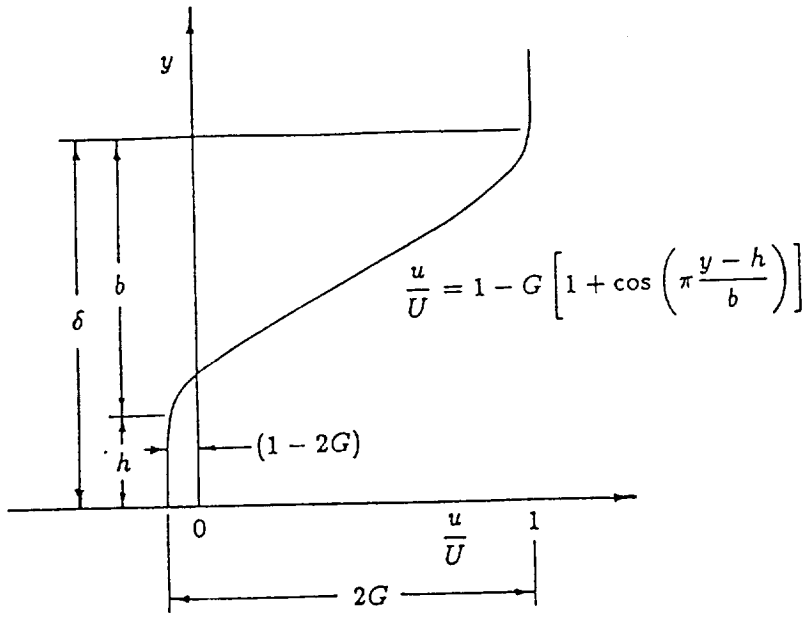

Fig. 5: Two-parameter reversed velocity profile of Green.[17]

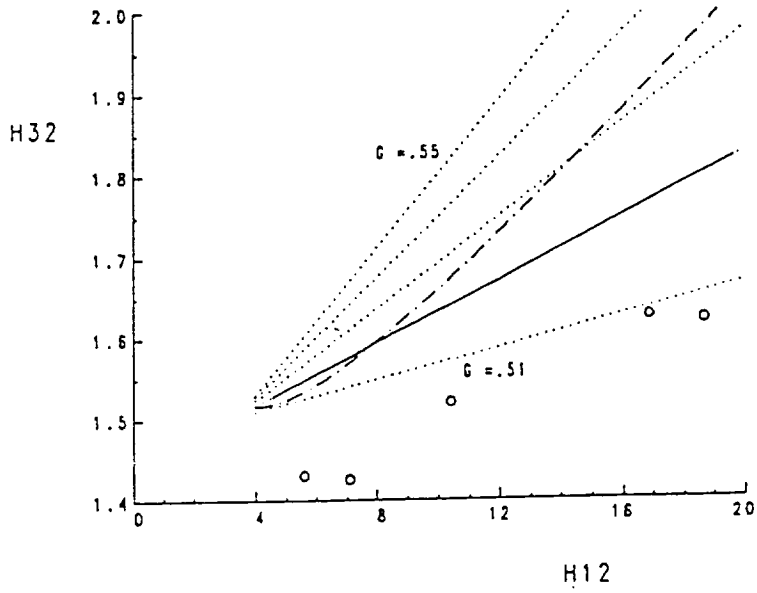

Fig. 6: Comparison of shape factor correlations. —·— : Ref. 5, from Stewartson profiles; ——— : Ref. 23, from fitted Green profiles; . . . : Eq. (9); o : measured, Ref. 23.

In the present separation bubble model, transition is predicted when a given value of the shape factor, $(H_{32})_T$, is achieved. As with other features of the bubble, $(H_{32})_T$ is taken to be dependent on both $(R_{\delta_2})_S$ and P. This relationship is

$$(H_{32})_T = \left[\frac{875 - (R_{\delta_2})_S}{35000000P^2 + 1800000P + 40000}\right]^{\frac{1}{3}} + 1.515095 \qquad (11)$$

To explain the transition criterion, it is plotted together with the shear layer development on the same plot that Eppler uses to describe the boundary-layer development.[7] Since H_{32} and R_{δ_2} are calculated at each point along the boundary layer, by connecting subsequent (H_{32}, R_{δ_2})-pairs on a plot whose axes correspond to these two variables, the boundary-layer development from the stagnation point to the trailing edge can be described in a very concise way. Fig. 8 shows one such boundary-layer development together with all the transition and separation criteria.

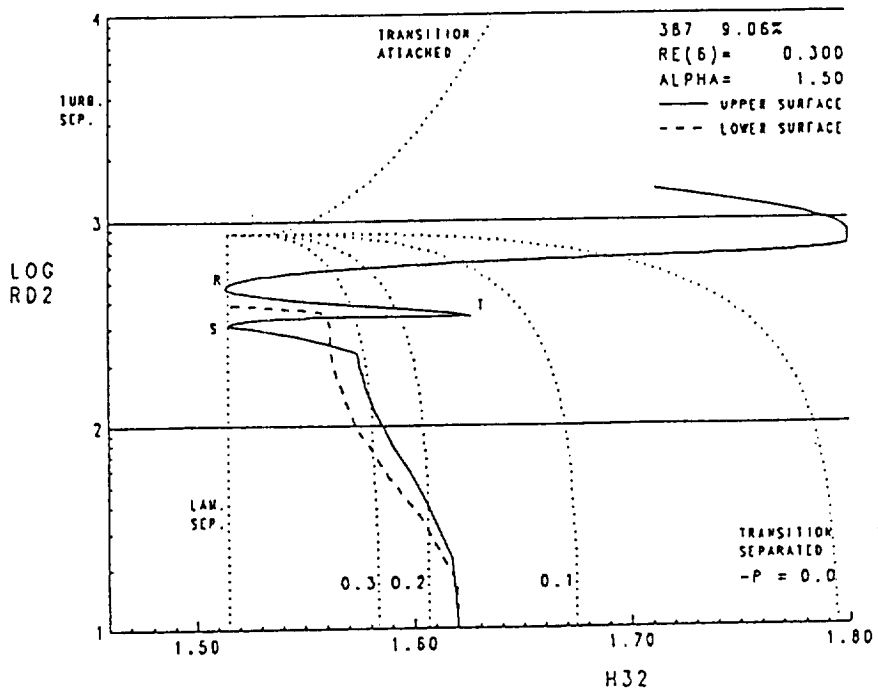

Fig. 8: Modified Eppler boundary-layer development plot showing the boundary-layer development inside the bubble.

Turbulent Part of the Bubble and Reattachment

An analysis recently completed by R. Eppler that establishes the greatest possible pressure recovery for an attached turbulent boundary layer provided inspiration for developing a new approach to the treatment of the turbulent part of the bubble. Given that the value as well as the slope of the H_{32} distribution is always known at the transition and reattachment points, a general function has been developed which allows the solution of the turbulent part of the bubble in the inverse mode. The distribution of H_{32} is specified as

$$H_{32}(\sigma) = \begin{cases} \frac{(H_{32})_T + (H_{32})_R}{2} + \frac{(H_{32})_T - (H_{32})_R}{2} \sin\left(\frac{\pi}{\frac{1.6}{6}\sigma + .4}\right) & 0 \le \sigma \le 1 \\ (H_{32})_R + A\left[1 + \sin\left(\frac{\pi}{\frac{1.6}{6}\sigma + .4}\right)\right] & \sigma > 1 \end{cases} \tag{12}$$

where

$$\sigma = \frac{s - s_T}{\ell_2} \tag{13}$$

The corresponding distributions of $U(s)$ and δ_2 are obtained from

$$\frac{dU}{ds} = \frac{H_{32}c_f - C_D + \delta_2 H'_{32}}{\delta_2 H_{32}(H_{12} - 1)} U \tag{14}$$

$$\frac{d\delta_2}{ds} = -\frac{3c_f}{H_{12} - 1} + \frac{H_{12} + 2}{(H_{12} - 1)H_{32}}(C_D - \delta_2 H'_{32}) \tag{15}$$

where H'_{32} denotes the derivative with respect to s of Eq. (12). The closure relations for separated and attached turbulent boundary layers developed by Drela[5] are used, enforcing continuity in H_{32} at transition.

In the expression defining the reattachment process, Eq. (12), there are two free constants, ℓ_2 and A, such that two additional conditions are necessary to achieve a unique solution. One condition is that the undershoot merge smoothly with the inviscid velocity distribution. Simultaneously, the reattachment condition derived by Horton[9] must be satisfied,

$$\left[\frac{\delta_2}{U}\frac{dU}{dx}\right]_R = -\left[\frac{C_D}{H_{32}(H_{12} - 1)}\right]_R \tag{16}$$

The accuracy of the self-consistent reattachment process described above depends on the choice of the function that represents the input H_{32} distribution and the value of $(H_{32})_T$. As the value of H_{32} at the end of the undershoot, which depends on the amplitude A, does not vary significantly with Reynolds number or pressure gradient, the function employed is believed to provide a satisfactory approximation to the actual boundary-layer development in the reattachment region as it is affected by the local interaction. Therefore, the only parameter requiring further calibration is $(H_{32})_T$. The transition criterion, Eq. (11), can be refined by matching predicted and measured pressure distributions. Having fixed $(H_{32})_T$, the correct dependence of G on P and, possibly, on $(R_{\delta_2})_S$, can be determined by matching predicted and measured transition lengths.

Predictions Based on the Present Bubble Model

At the present time, all of the components of the bubble model are in place with enough flexibility to capture the physics for a wide range of conditions. It remains, however, to determine the exact forms of the correlation functions that will "tune" the model to achieve the generality and robustness that this wide range requires. With these qualifications in mind, the pressure distribution for the Eppler E387 airfoil at an angle of attack of 1.5 degrees as predicted using the Eppler and Somers program with the bubble model included is shown in Fig. 9. Also included in the figure is the distribution obtained with the Drela and Giles program,[6] with a critical amplification factor of 12, along with that of McGhee et al.[21], both at 2 degrees. For this case, the predicted pressure distributions agree reasonably well with one another and with the experimental results. As expected, because this airfoil is not highly aft-loaded, the influence

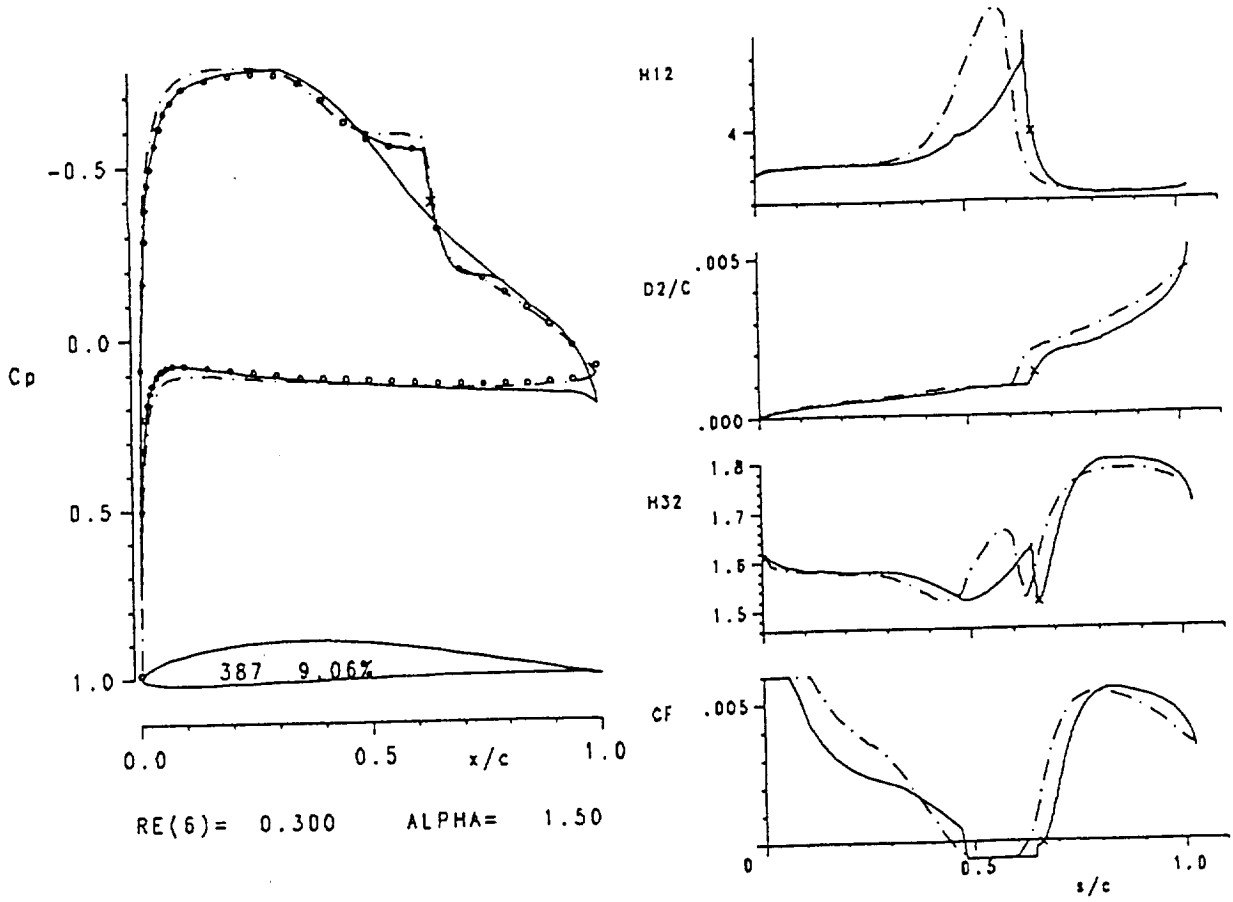

Fig. 9: Velocity distribution and upper-surface boundary-layer development predicted by present method compared to those of the Drela and Giles program.[6] Eppler E387 airfoil, $c_\ell = .55$. ——— : present method; — · — : method of Ref. 6; ○ : experimental, Ref. 21.

of viscous/inviscid interactions is not strong. Consequently, outside of the bubble region the inviscid prediction is comparable to that of the fully interactive method and, within the bubble region, the local interactive calculation of the present model produces results which are very close to those of the fully interactive method.

A comparison of the development of the boundary-layer properties for the E387 airfoil, H_{12}, δ_2, H_{32}, and c_f, calculated using the present method with those obtained using the Drela and Giles program are also presented in Fig. 9. As with the pressure distributions, the agreement between the predictions obtained using the present bubble model with those of the fully interactive method is good. The apparent difference in bubble length may be due to the different treatment of the transition region between the two methods. As in most transition prediction methods based on linear stability, the critical amplification factor used in the Drela and Giles program marks the beginning of the transition region while, in the present model, the transition point used corresponds to the end of this region and the beginning of the full turbulent calculations. The difference in the distribution of H_{32} can be attributed to the difference in pressure distributions in the laminar part of the bubble, shown in Fig. 9, as predicted by the two methods. The steeper pressure gradient predicted by the present model leads to a larger growth in δ_2 and, therefore, a smaller H_{32}.

The aerodynamic characteristics for the E387 airfoil, predicted using both the original and the modified Eppler and Somers program, are given in Fig. 10. Clearly, the drag predicted with the bubble model in use is much closer to the experimental values than that obtained without it. In fact, the largest difference between the two that is observed is less than four counts. In considering such plots, it should be noted that because the original program assumes transition at the laminar separation point, the width between the original transition development and that obtained with the modified program is the length of the laminar part of the bubble.

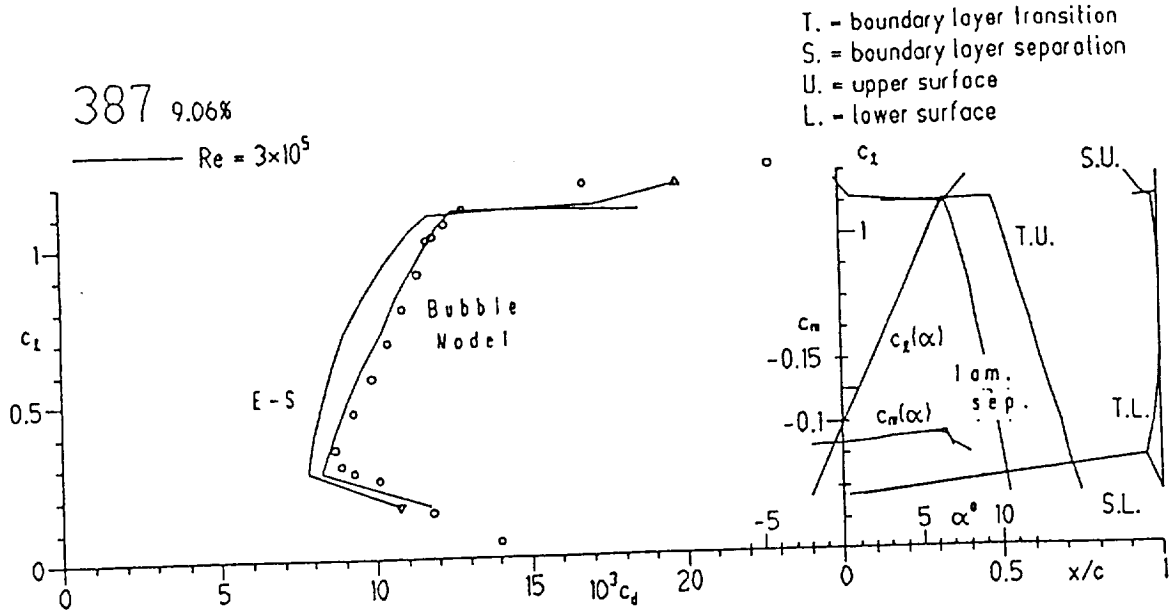

Fig. 10: Aerodynamic characteristics for the Eppler 387 airfoil obtained with the original Eppler and Somers program compared with those obtained using the program incorporating the present bubble model. Experimental data is from Ref. 21.

Because of the strong viscous interaction due to the large amount of aft-loading present, the NLF(1)-1015 airfoil represents a much more difficult case for the present method than does the E387 airfoil. The pressure distribution for this airfoil at an angle of attack relative to the chordline of -3.0 degrees is shown in Fig. 11. The greater impact of viscous interaction in this case compared to the last is apparent. While it should be emphasized again that the present model has yet to be fully calibrated, it is seen in this case that the overall method does seem to model the physical phenomenon sufficiently well to capture the two different bubble developments that occur on this airfoil at this angle of attack.

Concluding Remarks

While its development is still in progress, the laminar separation bubble model described seems to properly predict the behavior of the various parts of the bubble and possess the flexibility required to work over a wide range of cases. For some cases, such as those in which the viscous interactions greatly modify the inviscid pressure distribution, high accuracy in predicting the drag and the influence of the bubble clearly requires a fully interactive method. For many other cases, however, the present local interactive bubble model should provide a computationally efficient method which is well suited for the aerodynamic analysis which is required during the process of airfoil design.

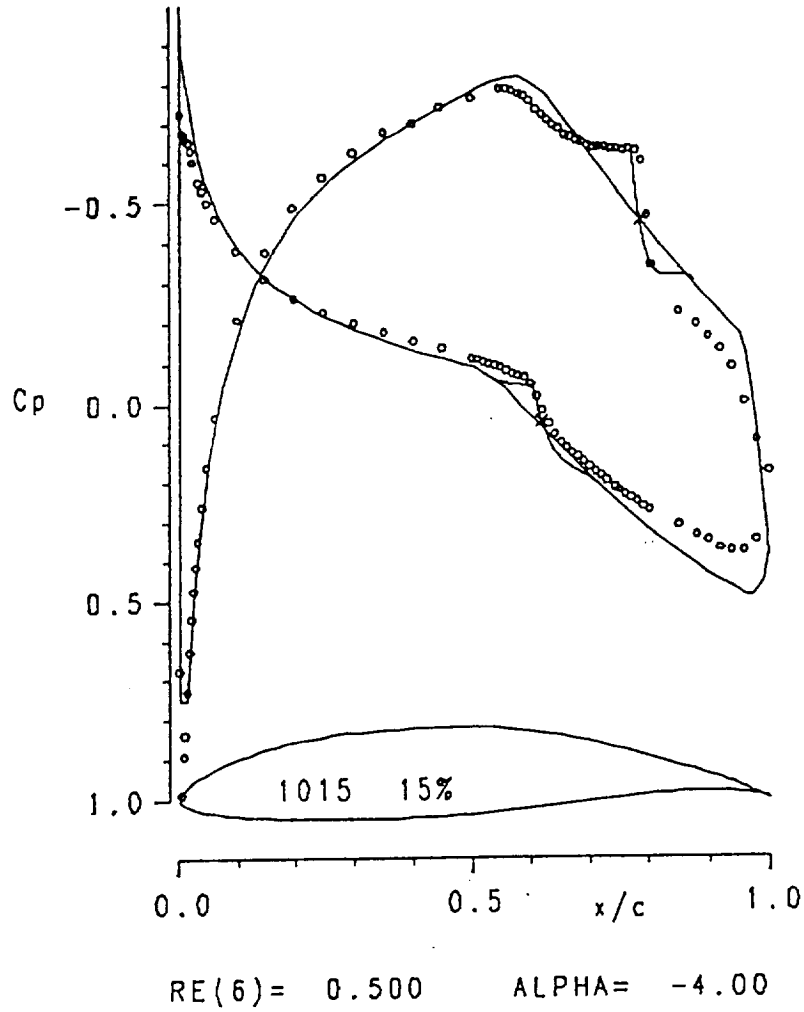

Fig. 11: Velocity distribution and boundary-layer development predicted by present method for NLF(1)-1015 airfoil, $c_\ell = .27$. o : experimental, NASA LaRC, June 1987.

Acknowledgements

This research was supported by the NASA Langley Research Center under Grant NAG 1-778. The authors also wish to acknowledge the contributions and support of the technical monitor, Mr. Dan M. Somers.

References

1. Mueller, T. J., "Low Reynolds Number Vehicles," AGARDograph No. 288, Feb. 1985.
2. Squire, H. B. and Young, A. D., "The Calculation of the Profile Drag of Aerofoils," Aeronautical Research Council R & M 1838, 1937.
3. Schmidt, G. S., "The Prediction of Transitional Separation Bubbles at Low Reynolds Numbers," Ph.D. Thesis, Department of Aerospace and Mechanical Engineering, University of Notre Dame, December 1986.
4. Davis, R. L. and Carter, J. E., "Analysis of Airfoil Transitional Separation Bubbles," NASA CR-3791, 1984.

5. Drela, M., "Two-Dimensional Transonic Aerodynamic Design and Analysis Using the Euler Equations," Massachusetts Institute of Technology, Gas Turbine Laboratory Report 187, February, 1986.
6. Drela, M. and Giles, M. B., "Viscous-Inviscid Analysis of Transonic and Low-Reynolds Number Airfoils," *AIAA Journal*, Vol. 25, No. 10, October, 1987, pp. 1347-1355.
7. Eppler, R. and Somers, D. M., "A Computer Program for the Design and Analysis of Low-Speed Airfoils," NASA TM-80210, 1980.
8. Eppler, R. "Recent Developments in Boundary Layer Computation," *International Conference on Aerodynamics at Low Reynolds Numbers* $10^4 < R < 10^6$, Vol. II, Royal Aeronautical Society, London, October 1986, pp. 12.1-12.18.
9. Horton, H. P., "A Semi-empirical Theory for the Growth and Bursting of Laminar Separation Bubbles," Aeronautical Research Council C. P. 1073, June 1967.
10. Roberts, W. B., "Calculation of Laminar Separation Bubbles and Their Effect on Airfoil Performance," *AIAA Journal*, Vol. 18, No. 1, January 1980, pp. 25-31.
11. Eppler, R. "Practical Calculation of Laminar and Turbulent Bled-Off Boundary Layers," NASA TM-75328, 1978. (Translated from *Ingenieur Archiv*, Vol. 32, 1963, pp. 221-245.)
12. Maughmer, M. D., "A Computationally Efficient Modelling of Laminar Separation Bubbles, Semi-Annual Status Report," NASA CR-182417, February 1988.
13. Dini, P. and Maughmer, M. D., "A Computationally Efficient Modelling of Laminar Separation Bubbles, Semi-Annual Status Report," February 1989.
14. Coton, F. N. and Galbraith, R. A. McD., "A Direct Aerofoil Performance Code Incorporating Laminar Separation Bubbles Effects," *Proceedings of the 16th Congress of the International Council of the Aeronautical Sciences*, ICAS 88-4.2.4, Vol. 1, 1988, pp. 329-338.
15. Gaster, M., "The Structure and Behaviour of Separation Bubbles," Aeronautical Research Council R. & M. No. 3595, March 1967.
16. Pauley, L. L., Moin, P., and Reynolds, W. C., "On the Structure of Two- and Three-Dimensional Separation," AIAA Paper No. 89-0287, January, 1989.
17. Green, J. E., "Two-Dimensional Turbulent Reattachment as a Boundary-Layer Problem," *Separated Flows*, AGARD Conference Proceedings No. 4, Part 1, May 1966.
18. Ingen, J. L. van, "On the Calculation of Laminar Separation Bubbles in Two-Dimensional Incompressible Flow," *Flow Separation*, AGARD Conference Proceedings No. 168, 1975.
19. Ingen, J. L. van and Boermans, L. M. M., "Aerodynamics at Low Reynolds Numbers: A Review of Theoretical and Experimental Research at Delft University of Technology," *International Conference on Aerodynamics at Low Reynolds Numbers* $10^4 < R < 10^6$, vol. I, Royal Aeronautical Society, London, October 1986, pp. 1.1-1.40.
20. Maughmer, M. D. and Somers, D. M., "Design and Experimental Results for a High-Altitude, Long-Endurance Airfoil," *Journal of Aircraft*, Vol. 26, No. 2, February 1989, pp. 148-153.
21. McGhee, R. J., Walker, B. S., and Millard, B. F., "Experimental Results for the Eppler 387 Airfoil at Low Reynolds Numbers in the Langley Low-Turbulence Pressure Tunnel," NASA TM-4062, October 1988.
22. Stewartson, K., "Further Solutions of the Falkner-Skan Equation," *Proceedings of the Cambridge Philosophical Society*, vol. 50, 1954, pp. 454-465.
23. Fitzgerald, E. J. and Mueller, T. J., "Laser Doppler Velocimeter Measurements of the Transitional Separation Bubble on an Airfoil at a Low Reynolds Number," to appear in *AIAA Journal*.